Journal of Mathematical Chemistry (© 2006)
DOI: 10.1007/s10910-006-9137-2

The undecakisicosahedral group and a 3-regular carbon network of genus 26

Erwin Lijnen* and Arnout Ceulemans
Departement Chemie, K.U.Leuven, Celestijnenlaan 200F, B-3001 Leuven, Belgium
Email: erwin.lijnen@chem.kuleuven.be

Patrick W. Fowler
Department of Chemistry, University of Sheffield, S3 7HF,UK

Michel Deza
Laboratoire de Géométrie Appliqué, LIGA-EuJC, École Normale Supérieure, 45 Rue d'Ulm, F-75230 Paris Cedex 05, France

Received 7 April 2006; revised 9 May 2006

Three projective special linear groups PSL(2,p), those with $p = 5, 7$ and 11, can be seen as p-multiples of tetrahedral, octahedral and icosahedral rotational point groups, respectively. The first two have already found applications in carbon chemistry and physics, as PSL(2,5) $\equiv I$ is the rotation group of the fullerene C_{60} and dodecahedrane $C_{20}H_{20}$, and PSL(2,7) is the rotation group of the 56-vertex all-heptagon Klein map, an idealisation of the hypothetical genus-3 "plumber's nightmare" allotrope of carbon. Here, we present an analysis of PSL(2,11) as the rotation group of a 220-vertex, all 11-gon, 3-regular map, which provides the basis for a more exotic hypothetical sp^2 framework of genus 26. The group structure and character table of PSL(2,11) are developed in chemical notation and a three dimensional (3D) geometrical realisation of the 220-vertex map is derived in terms of a punctured polyhedron model where each of 12 pentagons of the truncated icosahedron is connected by a tunnel to an interior void and the 20 hexagons are connected tetrahedrally in sets of 4.

KEY WORDS: PSL(2,11), group theory, undecakisicosahedral group, topology, carbon allotrope

AMS: 05C10, 20B25, 57M20

1. Introduction

The three groups PSL(2,5), PSL(2,7) and PSL(2,11) form a special subset of the Projective Special Linear groups PSL(2,p) in view of their particular

*Corresponding author.

permutational structure. They can be viewed as multiples of the symmetry groups of the regular polyhedra in three dimensional (3D) space, and for this reason are also called the pollakispolyhedral groups [1]. PSL(2,5) and PSL(2,7) correspond to the pentakistetrahedral, ${}^5T$, and heptakisoctahedral group, ${}^7O$, respectively. Both have found applications in chemistry and physics. PSL(2,5) is the rotation group of the icosahedron and of the skeleton of the most abundant fullerene, C_{60}. PSL(2,7) is the rotational symmetry of an idealisation of the "plumber's nightmare", which offers a model for "schwarzite" allotropes of carbon. This paper is devoted to the analysis of the third family member, PSL(2,11), which forms the undecakisicosahedral group, ${}^{11}I$. PSL(2,11), whilst perhaps more exotic than the first two groups, also describes trivalent frameworks and so has the potential for application to other hypothetical high-genus forms of carbon. We study the realization of ${}^{11}I$ as the symmetry group of a 60-vertex regular map of genus 26. The relationship between this map and the skeleton of C_{60} provides the key to this realization. Applications of PSL(2,11) in physics or chemistry so far are few. It has potential relevance for the study of the icosahedral phase of quasicrystals, [2] and was identified as a finite simple subgroup of the Cartan exceptional group E_8 [3]. The conjugacy class structure of the group has been used to provide a group theoretical specification of the C_{60} graph [4]. In view of the intrinsic connections between this group and the icosahedral lattice, sooner or later this powerful symmetry can be expected to appear directly in the description of physical phenomena.

2. The pollakispolyhedral groups

The concept of pollakispolyhedral groups arises from an alternative definition of the icosahedral rotation group I. Take p a prime number and let F_p denote the finite field of p elements. They can be represented by the elements $0, \ldots, p-1$; larger elements can be reduced to an element in this finite field by dividing by p and taking the remainder. The set of all 2×2 matrices with all entries in the field F_p and determinant 1 then forms a group which is known in mathematics as the special linear group SL(2,p) [5]. It has order $p(p^2-1)$. The group PSL(2,p) is defined as the quotient group of SL(2,p) modulo its centre, where this centre consists of all scalar matrices. For all prime numbers $p \geqslant 5$, the centre has only two elements and the corresponding quotient group PSL(2,p) is simple. Of all these prime numbers p however, the numbers $p = 5, 7, 11$ stand out as they are the only cases in which the group PSL(2,p) acts transitively on sets of p as well as on sets of $p+1$ elements, a result already known to Galois. For all other prime values of p the group PSL(2,p) acts transitively on sets of $p+1$ elements, but not on sets of p elements. In this way, the three projective linear groups PSL(2,5), PSL(2,7) and PSL(2,11) are distinguished from the rest and form a special family known as the pollakispolyhedral groups.

The smallest member PSL(2,5) has 60 elements and is isomorphic to the pure icosahedral rotation group I. It is alternatively called the pentakistetrahedral group ${}^5T$ as it contains the tetrahedral group as a subgroup of index 5. This can easily be seen on a regular dodecahedron where the 20 vertices can be divided into five sets of four vertices such that each set of four vertices forms a regular tetrahedron [1]. The group PSL(2,5) acts transitively on this set of five tetrahedra by the action of one of the fivefold rotations. The group acts also transitively on a six element set as can be seen from the action on the six diagonals of the regular icosahedron connecting opposite points.

A similar analysis can be made for the group PSL(2,7) of order 168, which is alternatively called the heptakisoctahedral group ${}^7O$ as it contains the octahedral group O as a subgroup of index 7. The group can be represented by the regular genus-3 Klein map, named after Felix Klein who investigated its very high symmetry in connection with the theory of multivalued functions [6]. Using this map it is easy to show the transitive character on a 7-set, as under removal of the sevenfold symmetry elements, the 56 vertices split into seven octahedral structures containing eight vertices. The complete structure of this group and its relevance to some negative-curvature carbon structures was described in previous papers [1,7].

As we shall see, the last member of the pollakispolyhedral groups, the undecakisicosahedral group ${}^{11}I$ or PSL(2,11), can also be represented by means of a regular map. The smallest 3-regular map with rotational symmetry PSL(2,5) (i.e., ${}^5T$ or I) is the all-pentagon dodecahedral map, and the smallest with the rotational symmetry PSL(2,7) (i.e., ${}^7O$) is the all-heptagon Klein map. Likewise, to realise PSL(2,11) (i.e., ${}^{11}I$) by a 3-regular map it is necessary to go to an all-undecagon map which will have 220 vertices, v, and 330 edges, e and 60 faces, f. Hence, from $f = v/2 + 2(1 - g)$, we find a genus g of 26. Conder and Dobcsányi [8] have tabulated all the small 3-regular maps, and the map of interest here is F220A in their catalogue. An explicit adjacency list for this graph was supplied to us by Professor Conder. Its total automorphism group consists of 1,320 elements, of which the orientation-preserving (rotational) part of 660 elements corresponds with the group PSL(2,11). While the genus-3 Klein map can still be visualized as a triply periodic structure in 3D space, [1] a geometrical representation for this genus-26 map has thus far not yet been reported. The most obvious representation would be to draw a Schlegel-like diagram consisting of a central 11-gon surrounded by layers of undecagonal faces, adding layers until all faces have been accounted for. In figure 1, we show such a central 11-gon surrounded by its eleven neighbouring faces together with an indication of the next layer of faces. Continuation to produce the whole diagram with 220 numbered vertices and all 60 faces would yield a very intricate figure. Instead, we work with the dual map, represented by the dashed lines in figure 1. It consists of 60 undecavalent vertices and 220 triangular faces, and of course retains the PSL(2,11)

Table 1
Rotation-scheme of the 60-vertex dual map, which is used to give a geometrical representation of the group PSL(2,11).

1.	5	43	32	31	37	48	18	39	2	57	58	31.	35	21	7	6	4	50	37	1	32	26	27
2.	1	39	53	52	33	44	24	35	3	56	57	32.	31	1	43	42	8	22	60	10	33	30	26
3.	2	35	49	48	54	40	30	51	4	60	56	33.	32	10	46	50	44	2	52	41	34	29	30
4.	3	51	45	44	50	31	6	47	5	59	60	34.	33	41	23	22	47	6	20	49	35	28	29
5.	4	47	36	40	41	52	12	43	1	58	59	35.	34	49	3	2	24	42	15	21	31	27	28
6.	10	57	16	20	34	47	4	31	7	53	54	36.	40	5	47	46	27	16	56	29	37	24	25
7.	6	31	21	25	17	58	29	19	8	52	53	37.	36	29	55	54	48	1	31	50	38	23	24
8.	7	19	48	47	22	32	42	24	9	51	52	38.	37	50	17	16	51	30	14	53	39	22	23
9.	8	24	59	58	49	20	39	46	10	55	51	39.	38	53	2	1	18	46	9	20	40	21	22
10.	9	46	33	32	60	25	13	57	6	54	55	40.	39	20	26	30	3	54	41	5	36	25	21
11.	15	42	54	53	59	26	19	56	12	50	46	41.	45	23	34	33	52	5	40	54	42	17	18
12.	11	56	22	21	55	43	5	52	13	49	50	42.	41	54	11	15	35	24	8	32	43	16	17
13.	12	52	27	26	23	57	10	25	14	48	49	43.	42	32	1	5	12	55	28	14	44	20	16
14.	13	25	44	43	28	53	38	30	15	47	48	44.	43	14	25	24	2	33	50	4	45	19	20
15.	14	30	58	57	45	21	35	42	11	46	47	45.	44	4	51	55	21	15	57	23	41	18	19
16.	20	6	57	56	36	27	51	38	17	42	43	46.	50	33	10	9	39	18	27	36	47	15	11
17.	16	38	50	49	58	7	25	60	18	41	42	47.	46	36	5	4	6	34	22	8	48	14	15
18.	17	60	28	27	46	39	1	48	19	45	41	48.	47	8	19	18	1	37	54	3	49	13	14
19.	18	48	8	7	29	56	11	26	20	44	45	49.	48	3	35	34	20	9	58	17	50	12	13
20.	19	26	40	39	9	49	34	6	16	43	44	50.	49	17	38	37	31	4	44	33	46	11	12
21.	25	7	31	35	15	45	55	12	22	39	40	51.	55	45	4	3	30	38	16	27	52	8	9
22.	21	12	56	60	32	8	47	34	23	38	39	52.	51	27	13	12	5	41	33	2	53	7	8
23.	22	34	41	45	57	13	26	59	24	37	38	53.	52	2	39	38	14	28	59	11	54	6	7
24.	23	59	9	8	42	35	2	44	25	36	37	54.	53	11	42	41	40	3	48	37	55	10	6
25.	24	44	14	13	10	60	17	7	21	40	36	55.	54	37	29	28	43	12	21	45	51	9	10
26.	30	40	20	19	11	59	23	13	27	31	32	56.	60	22	12	11	19	29	36	16	57	2	3
27.	26	13	52	51	16	36	46	18	28	35	31	57.	56	16	6	10	13	23	45	15	58	1	2
28.	27	18	60	59	53	14	43	55	29	34	35	58.	57	15	30	29	7	17	49	9	59	5	1
29.	28	55	37	36	56	19	7	58	30	33	34	59.	58	9	24	23	26	11	53	28	60	4	5
30.	29	58	15	14	38	51	3	40	26	32	33	60.	59	28	18	17	25	10	32	22	56	3	4

rotational symmetry of the original 220-vertex 3-regular map. A full description of this dual map is by means of a rotation scheme (table 1) [9]. Such a scheme lists for every vertex of the map a consistent cyclic rotation (called a local rotation) of the edges emanating from this vertex listed by the end-vertices. For instance, for vertex **1**[1] one sees that going around this vertex, one first encounters the edge (**1–5**), followed by (**1-43**), ... and eventually (**1–58**). The faces can be retrieved by the face-tracing procedure as discussed in [9]. In the present case, identification of all triangular faces is a trivial task as each triple composed of a vertex and two consecutive vertices in its local rotation forms a

[1]Throughout, vertex labels are in bold.

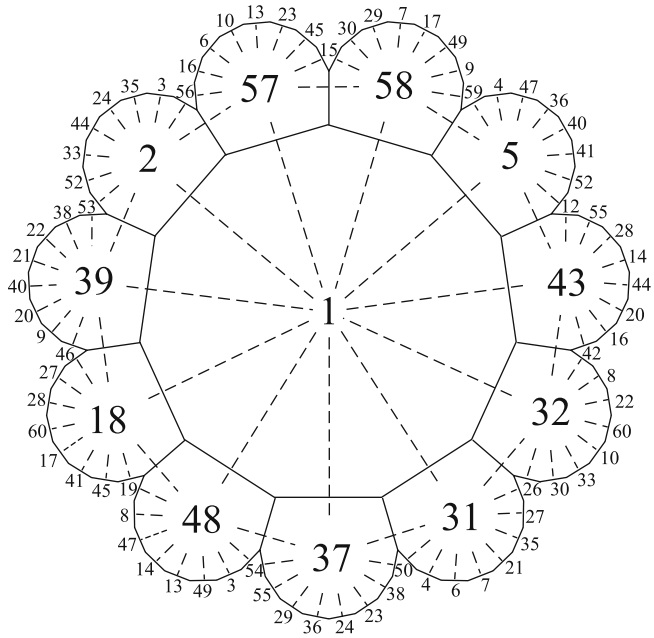

Figure 1. Partial Schlegel-like diagram representing the 220-vertex regular map of genus 26. The face-numbering corresponds with the numbering used in table 1 to describe the 60-vertex dual map. The edges of the dual map are drawn as dashed lines.

face. Our final aim is to replace this combinatorial representation with a geometrical one which makes it possible to locate the 26 handles of the map. First, we analyse the structure of the highly symmetrical undecakisicosahedral group.

3. The undecakisicosahedral group

3.1. Conjugacy-classes

In this section, we describe in detail the group structure and representations of the undecakisicosahedral group ${}^{11}I$. The 660 elements are subdivided into eight conjugacy classes:

$$ {}^{11}I = E + 60C_{11} + 60C_{11}^2 + 110C_3 + 55C_2 + 132C_5 + 132C_5^2 + 110C_6. \qquad (1) $$

As indicated before, these group-elements can most easily be represented as the orientation-preserving automorphisms of the regular genus-26 dual map (figure 1). As it is a regular map, its rotational symmetry group ${}^{11}I$ can be generated by only two generators, [10] in this case an 11-fold symmetry operation through one of the undecavalent vertices and a threefold symmetry operation through

one of the triangular faces. A C_{11}-type generator can be visualized on the Schlegel-diagram of figure 1. It is obtained by performing an 11-fold rotation through the central vertex **1**, leading to the following permutation:

$$\begin{aligned} C_{11} \rightarrow\ & (1), (11), (25), (34), (51), \\ & (2, 57, 58, 5, 43, 32, 31, 37, 48, 18, 39), \\ & (3, 45, 9, 52, 16, 30, 4, 55, 8, 27, 38), \\ & (6, 29, 47, 28, 22, 35, 23, 49, 41, 20, 33), \\ & (7, 36, 14, 60, 21, 24, 13, 17, 40, 44, 10), \\ & (12, 42, 26, 50, 54, 19, 46, 53, 56, 15, 59). \end{aligned} \tag{2}$$

Notice that although, we have chosen to adopt a point group notation for this symmetry element, it does not correspond to an ordinary 11-fold rotation operation. In fact, the C_{11} operation stabilizes five vertices, giving a total of $60/5 = 12$ 11-fold directions. Notice also that these stabilized vertices and their surroundings are not rotated through the same angle. When the C_{11} operation of eq. (2) rotates vertex **1** through $2\pi/11$, vertex **11** is rotated through $3 \times 2\pi/11$, **25** $\rightarrow 4 \times 2\pi/11$, **34** $\rightarrow\ 9 \times 2\pi/11$ and **51** $\rightarrow 5 \times 2\pi/11$. The elements C_{11}, C_{11}^3, C_{11}^4, C_{11}^5 and C_{11}^9 are therefore in one class, containing a total of $12 \times 5 = 60$ elements. The other class of 60 11-fold elements is similarly formed by the remaining powers of C_{11}, namely C_{11}^2, C_{11}^6, C_{11}^7, C_{11}^8 and C_{11}^{10}. We can take as a threefold generator the C_3 element going through the triangular face (**1,2,57**), which reads:

$$\begin{aligned} C_3 \rightarrow\ & (1, 2, 57), (3, 15, 18), (4, 14, 27), (5, 53, 16), (6, 43, 52), \\ & (7, 20, 12), (8, 34, 55), (9, 22, 29), (10, 32, 33), (11, 17, 40), \\ & (13, 31, 44), (19, 49, 21), (23, 37, 24), (25, 26, 50), (28, 51, 47), \\ & (30, 46, 60), (35, 45, 48), (36, 59, 38), (39, 56, 58), (41, 54, 42). \end{aligned} \tag{3}$$

In total four triangular faces are stabilized by this C_3 element: (**1**, **2**, **57**), (**41**, **54**, **42**), (**10**, **33**, **32**) and (**23**, **24**, **37**), where the first two faces are rotated clockwise through $2\pi/3$ and the last two faces counterclockwise through $2\pi/3$. The inverse element C_3^{-1} therefore belongs to the same class, giving a total of $(220/4) \times 2 = 110$ threefold elements. C_{11} and C_3 generators can be combined to yield a C_2 operation in the following way:

$$\begin{aligned} C_2 = C_3 \times C_{11} \rightarrow\ & (1, 2), (3, 48), (4, 8), (5, 52), (6, 9), (7, 59), \\ & (10, 20), (11, 17), (12, 41), (13, 40), (14, 30), (15, 38), \\ & (16, 46), (18, 56), (19, 60), (21, 23), (22, 45), (24, 31), \\ & (25, 26), (27, 36), (28, 29), (32, 44), (33, 43), (34, 55), \\ & (35, 37), (39, 57), (42, 50), (47, 51), (49, 54), (53, 58). \end{aligned} \tag{4}$$

This agrees with the fact that three adjacent symmetry elements in a regular map combine to form the unit element, $C_3 \times C_{11} \times C_2 = E$ [11]. The C_2 operation is seen to leave six edges invariant: (**1**, **2**), (**3**, **48**), (**5**, **52**), (**14**, **30**), (**27**, **36**), (**28**, **29**). In this way, the 330 edges of our map give rise to a total of 330/6=55 twofold elements. Further, one also has sixfold elements C_6, which are located along the same directions as the C_3 axes:

$$\begin{aligned} C_6 \rightarrow\ & (1, 42, 2, 41, 57, 54), (3, 5, 15, 53, 18, 16), \\ & (4, 47, 14, 28, 27, 51), (6, 48, 43, 35, 52, 45), \\ & (7, 19, 20, 49, 12, 21), (8, 44, 34, 13, 55, 31), \\ & (9, 50, 22, 25, 29, 26), (10, 37, 32, 24, 33, 23), \\ & (11, 39, 17, 56, 40, 58), (15, 53, 18, 16, 3, 5). \end{aligned} \tag{5}$$

Each of the 10 composing six-cycles can be seen as a kind of rotation-reflection, which connects two three-cycles of the corresponding C_3 element. As the inverse elements C_6^{-1} are part of the same class, it contains a total of 110 elements. The square and cubic powers correspond to the previously discussed C_3 and C_2 elements. Finally, the two remaining classes consist of five-fold symmetry elements, which group the 60 vertices together in 12 5-cycles:

$$\begin{aligned} C_5 \rightarrow\ & (1, 39, 20, 6, 31), (2, 40, 16, 7, 32), (3, 36, 17, 8, 33), \\ & (4, 37, 18, 9, 34), (5, 38, 19, 10, 35), (11, 13, 15, 12, 14), \\ & (21, 43, 53, 26, 57), (22, 44, 54, 27, 58), (23, 45, 55, 28, 59), \\ & (24, 41, 51, 29, 60), (25, 42, 52, 30, 56), (46, 49, 47, 50, 48). \end{aligned} \tag{6}$$

Their interpretation will become clearer in the next section when we give a new geometrical representation to locate the 26 handles of our map. Here, we limit ourselves to stating that there are a total of 66 fivefold directions, which give rise to a 132-element class consisting of the C_5 elements and their inverses C_5^4, and a class of 132 elements formed by the C_5^2 elements and their inverse operations C_5^3.

3.2. Character table

In table 2, we show the character table of ${}^{11}I$, which was retrieved from the Atlas of Finite Groups [5]. The notation of its irreducible representations has however been adapted to a chemical notation based on their representational degeneracy: A is non-degenerate, E and T doubly and triply degenerate, G and H fourfold and fivefold degenerate, and from then on higher degeneracies are indicated in alphabetical order (I, J, K, L, M, N, O, ...). There are eight irreducible representations, with labels A, H_1, H_2, M_1, M_2, N, O_1 and O_2. We thus have

Table 2
Character table of ${}^{11}I$.

	E	$55C_2$	$110C_3$	$132C_5$	$132C_5^2$	$110C_6$	$60C_{11}$	$60C_{11}^2$
A	1	1	1	1	1	1	1	1
H_1	5	1	−1	0	0	1	A	A*
H_2	5	1	−1	0	0	1	A*	A
M_1	10	−2	1	0	0	1	−1	−1
M_2	10	2	1	0	0	−1	−1	−1
N	11	−1	−1	1	1	−1	0	0
O_1	12	0	0	B	B**	0	1	1
O_2	12	0	0	B**	B	0	1	1

$A = 1/2(-1 + i\sqrt{11})$; $B = 12(-1 + \sqrt{5})$.

a non-degenerate representation and two fivefold, two tenfold, one 11-fold and two 12-fold degeneracies. A single asterisk denotes a complex conjugate. The H_1 and H_2 representations therefore form a complex conjugate pair. The entries B and B^{**} are also connected as irrational conjugates under $\sqrt{5} \to -\sqrt{5}$.

3.3. Subgroup structure

In this section, we discuss the subgroup structure of ${}^{11}I$, which will be of importance in the next section, where we try to find a geometrical model for our genus-26 map. Figure 2 gives the full genealogical tree of ${}^{11}I$, where the lines indicate direct group-subgroup lineage. It was retrieved from a generator-based program [9]. As we can see, our parent group has four direct subgroups: I', I'', $M_{5,11}$ and D_6. In total there are 22 subgroups isomorphic to the purely rotational icosahedral group. They fall into two subgroup classes I' and I'', which are non-equivalent within ${}^{11}I$ symmetry. The subgroups within one of these classes are transformed into each other by any one of the 11-fold operations. Note, that equivalence of both classes is restored when one considers the full symmetry group ${}^{11}I_d$ of the genus-26 map, which also includes orientation-reversing symmetry operations. The second largest subgroup class consists of 12 groups of order 55 corresponding with the metacyclic group $M_{5,11}$, which is formed by the semi-direct product of a fivefold and 11-fold cyclic group and is the only subgroup of ${}^{11}I$ that is not isomorphic with a point group. The fourth direct subgroup class contains 55 groups of order 12 isomorphic to a sixfold dihedral group. Apart from the subgroup class T with 55 purely rotational tetrahedral groups, all other subgroup classes are only composed of dihedral groups D_n or cyclic groups C_n.

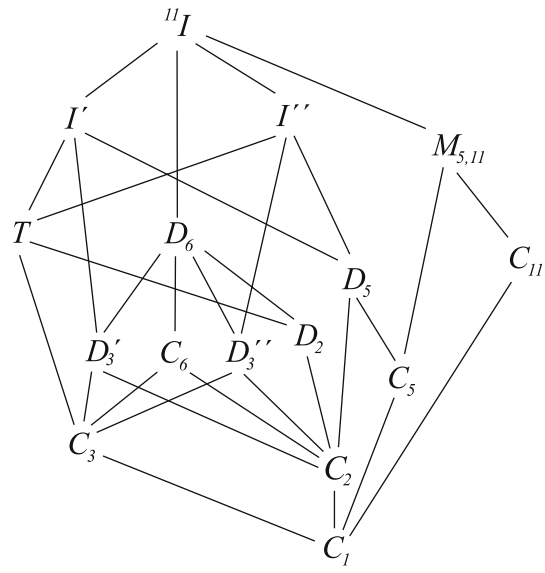

Figure 2. Genealogical tree of subgroups of the undecakisicosahedral group ^{11}I.

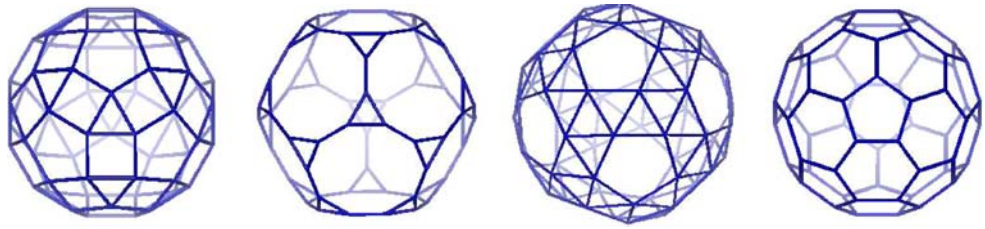

Figure 3. The four icosahedral Archimedean solids on 60 vertices. From left to right: the small rhombicosidodecahedron, the truncated dodecahedron, the snub dodecahedron and the truncated icosahedron.

4. Geometrical realization of ^{11}I

In this section, we will look for a good geometrical model for our 60-vertex map, one that makes it possible to locate the 26 handles and thereby interpret its intricate topology. In the previous section, we saw that the group ^{11}I contains the purely rotational icosahedral group I as the highest subgroup with point group symmetry. We therefore investigate the possibility of forming a 3D geometrical model exhibiting such icosahedral symmetry, where we further impose the restriction that the 60 vertices remain equivalent, as is the case under PSL(2,11) symmetry. In 3D space there are four semiregular convex polyhedra on 60 vertices obeying these restrictions. They are the four icosahedral Archimedean solids on 60 vertices depicted in figure 3, namely the small

Table 3
Some properties of the four Archimedean solids on 60 vertices. f_i is the number of faces of size i.

Solid	v	e	f	f_3	f_4	f_5	f_6	f_{10}
Small rhombicosidodecahedron	60	120	62	20	30	12	–	–
Truncated dodecahedron	60	90	32	20	–	–	–	12
Snub dodecahedron	60	150	92	80	–	12	–	–
Truncated icosahedron	60	90	32	–	–	12	20	–

rhombicosidodecahedron, the truncated dodecahedron, the snub dodecahedron and the truncated icosahedron. In table 3, we list some of their properties.

Seeking a geometrical representation it is worth investigating whether the graphs of these Archimedean solids appear as subgraphs of the graph underlying our 26-genus map. If such an Archimedean subgraph does indeed exist, it would be useful as a 3D icosahedral backbone on which a complete geometrical model of the genus-26 map could be built. In general, the search for a specific subgraph within a given graph is an NP-complete problem [12]. In the present case however, we want the point group of the Archimedean graph to be one of the 22 icosahedral subgroups of the parent group ${}^{11}I$. Any one of the 22 can be taken, as all will merge into a single class under the total symmetry group of our map ${}^{11}I_d$ (including both orientation preserving and orientation reversing automorphisms). As icosahedral subgroup we have chosen the group generated by the following five and threefold elements:

$$
\begin{aligned}
C_5 \rightarrow\ & (1, 2, 3, 4, 5), (6, 12, 18, 24, 30),\\
& (7, 13, 19, 25, 26), (8, 14, 20, 21, 27),\\
& (9, 15, 16, 22, 28), (10, 11, 17, 23, 29),\\
& (31, 52, 48, 44, 40), (32, 53, 49, 45, 36),\\
& (33, 54, 50, 41, 37), (34, 55, 46, 42, 38),\\
& (35, 51, 47, 43, 39), (56, 60, 59, 58, 57),
\end{aligned}
$$

$$
\begin{aligned}
C_3 \rightarrow\ & (1, 17, 24), (2, 18, 25), (3, 19, 21), (4, 20, 22),\\
& (5, 16, 23), (6, 34, 47), (7, 35, 48), (8, 31, 49),\\
& (9, 32, 50), (10, 33, 46), (11, 55, 30), (12, 51, 26)\\
& (13, 52, 27), (14, 53, 28), (15, 54, 29), (36, 57, 41)\\
& (37, 58, 42), (38, 59, 43), (39, 60, 44), (40, 56, 45). \qquad (7)
\end{aligned}
$$

Our strategy to identify the Archimedean subgraphs with this symmetry consists in taking an arbitrary vertex (all 60 vertices are equivalent) and build an Archimedean framework, using a triple of neighbouring icosahedral symmetry elements to generate the chosen icosahedral group. Each time new vertices

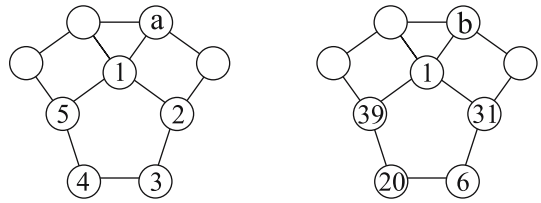

Figure 4. Small patches of the small rhombicosidodecahedron consisting of all faces surrounding vertex **1** and depicting the cases with the starting pentagon (**1**, **2**, **3**, **4**, **5**) (Left) and (**1**,**31**,**6**,**20**,**39**) (Right).

are added, a check is made that the partial structure still complies with the connectivity of our genus-26 graph. In the following subsections we will investigate case-by-case the existence/non-existence of each of the four types of icosahedral Archimedean subgraphs.

4.1. The Small rhombicosidodecahedron

In figure 4, we depict the local environment around a starting vertex, say **1**, of the small rhombicosidodecahedron. This vertex is seen to be surrounded by a pentagonal, a triangular and two quadrangular faces. As there is a fivefold axis running through the centre of the pentagonal face, we can start by identifying all possible pentagonal cycles containing vertex **1**. To comply with the imposed icosahedral symmetry, the next nearest neighbours of vertex **1** within such a pentagonal cycle must be images of vertex **1** under some fivefold operation (C_5 or C_5^2) of the above defined icosahedral subgroup. We therefore identify all images of vertex **1** under the operations of both conjugacy classes. They are found by explicit generation of the icosahedral group of 60-vertex permutations defined by the generators of eq. (7):

$$\begin{aligned} \mathbf{1} &\xrightarrow{C_5\text{–type operations}} \mathbf{2}/\mathbf{5}/6/10/11/15/16/20/21/25/26/30, \\ \mathbf{1} &\xrightarrow{C_5^2\text{–type operations}} 3/4/\mathbf{31}/34/36/\mathbf{39}/41/44/46/49/54. \end{aligned} \tag{8}$$

In this way, we get a listing of all *possible* neighbours of vertex **1** in the unique pentagonal cycle containing this vertex. However, following the rotation scheme of table 1, we see that of these images, only the vertices indicated in bold on the right of eq. (9) are neighbours of vertex **1**. They define two different pentagonal cycles. The first cycle (**1**, **2**, **3**, **4**, **5**), is defined by an element of the C_5 class, the second (**1**,**31**,**6**,**20**,**39**) transforms by an element of the C_5^2 class. We therefore have to distinguish two cases, depending on the chosen starting pentagon.

We start with pentagon (**1**, **2**, **3**, **4**, **5**) (figure 4, left). As the quadrangular cycles are crossed by twofold axes, we can use the images of vertex **2** under the 15 twofold elements to identify the possible vertices for position a.

$$\mathbf{2} \xrightarrow{C_2\text{–type operations}} 9/14/19/24/29/31/36/41/46/51\ 56/57/58/59/60. \tag{9}$$

Of these images, only the vertices **31**, **57** and **58** are also neighbours of vertex **1** and can therefore occupy position a. However, because there is a threefold axis running through the trigonal cycle, the vertex at position a should also be an image of vertex **1** under one of the 20 threefold elements.

$$\mathbf{1} \xrightarrow{C_3\text{–type operations}} 7/9/12/14/17/19/22/24/27/29\ 32/33/37/38/42/43/47/48/52/53. \tag{10}$$

The above list however shows that none of the three candidates for position a are images of **1** under a C_3-type operation. It is therefore, impossible to find a vertex for position a under the defined icosahedral subgroup, and the left-hand starting configuration of figure 4 cannot be extended to a small rhombicosidodecahedral subgraph.

For the case with the starting pentagon (**1**,**31**,**6**,**20**,**39**) (figure 4, right), the possible vertices at position b can be found in a similar way, now looking at the images of vertex **31** under the twofold operations.

$$\mathbf{31} \xrightarrow{C_2\text{–type operations}} 2/10/11/17/23/26/27/28/29/30\ 37/45/47/55/59. \tag{11}$$

Of these images, only the vertices **2** and **37** are neighbours of vertex **1**, but vertex **2** is not an image of vertex **1** under any of the threefold operations, so we are only left with vertex **37** for position b. The triple of incident five, three and twofold operations through the faces neighbouring vertex **1** are now uniquely identified and as they form a generating set, they can be used to reconstruct the remaining part of the small rhombicosidodecahedral structure. The resulting structure is shown in figure 5 and it can be easily checked from table 1 that it is a valid subgraph. Now that, we have found this unique small rhombicosidodecahedral subgraph, we can use it as a backbone for an icosahedral representation of our genus-26 map. It remains to add the seven missing connectivities for each vertex as prescribed by the rotation scheme of table 1. However, as all 60 vertices are equivalent, we need not reconstruct the whole map but instead only a small patch of all faces surrounding vertex **1** (figure 6). Of the seven missing connections emanating from vertex **1** there is one to the inside

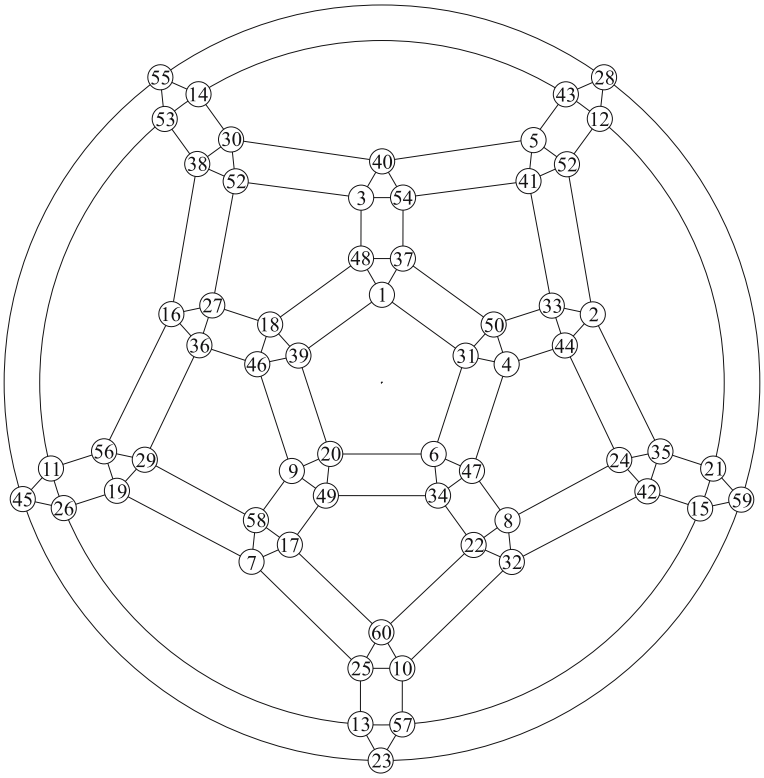

Figure 5. Schlegel diagram of the unique small rhombicosidodecahedral subgraph of the genus-26 map.

of the square (**1**,**39**,**18**,**48**) and the other six are all to the inside of the pentagon (**1**,**31**,**6**,**20**,**39**). The squares are thus nicely triangulated and, just as the triangles, form completely closed entities without holes, thereby not contributing to the overall topology of our genus-26 map. The 26 handles are thus confined to the set of 12 pentagons, which are mutually connected in an intricate way, making it very difficult to visualise this topology in 3D space. The possible existence of the other types of Archimedean subgraphs is therefore investigated.

4.2. The truncated dodecahedron

As in the previous section, we are to try to find the possible truncated dodecahedral subgraphs using a triple of mutually adjacent five-, three- and twofold axes of our chosen icosahedral group. Figure 7 shows a small patch of the local environment around vertex **1**, consisting of two decagonal and one triangular face. As a fivefold axis through the decagonal face does not map neighbouring vertices onto each other, we choose to start from the threefold axis through

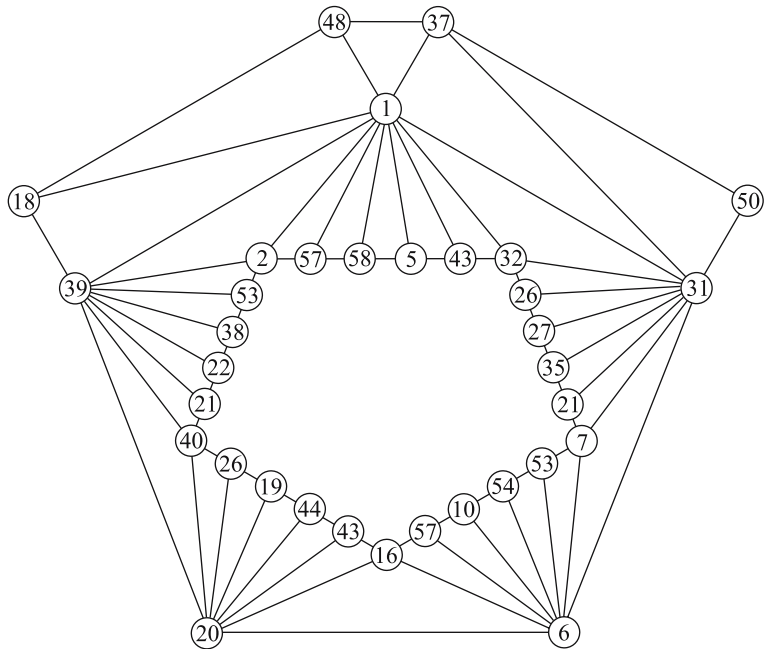

Figure 6. Small patch taken from the small rhombicosidodecahedral subgraph of figure 5 showing the structure of the genus-26 map around vertex **1**.

the triangle containing vertex **1**. From eq. (10) and table 1, we find that only the vertices **32**, **37**, **43** and **48** are both images of **1** under a threefold operation and neighbours of **1**. Together they define two possible starting triangles, (**1**,**43**,**32**) and (**1**,**37**,**48**). For the first starting triangle (**1**,**43**,**32**) (figure 7, left), we can use the images of vertex **1** under the twofold operations to identify the unknown neighbour of vertex **1**.

$$\mathbf{1} \xrightarrow{C_2\text{–type operations}} 8/13/18/23/28/35/40/45/50/55\ 56/57/58/59/60. \tag{12}$$

Of these images, only the vertices **57**, **58** and **18** are neighbours of vertex **1**. We have thus identified three candidate C_2-operations, which can also be used to determine the vertices at positions d and e, as they form the images of vertex **32** and **43**, respectively. On the left-hand side of figure 7, the three possible situations are depicted by the numbers in the circles, squares and diamonds. The situation with vertex **18** as a neighbour of vertex **1** (diamonds) can be excluded as there is no fivefold symmetry element that maps vertex **1** onto vertex **28** (See eq. (9)). The other two cases (circles and squares) comply with our chosen icosahedral symmetry and can both be extended to a truncated dodecahedral subgraph. However, neither is useful for visualisation. As the triangular

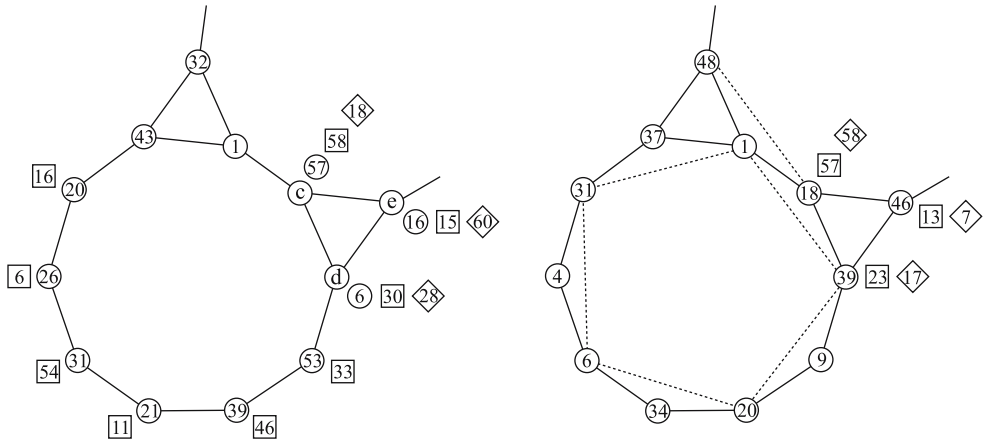

Figure 7. Patches, which can be used to build complete truncated dodecahedral subgraphs starting from the triangle (**1**, **43**, **32**) (Left) and the triangle (**1**, **37**, **48**) (Right).

faces of both truncated dodecahedral subgraphs are faces of the genus-26 map, they are completely closed and have no contribution to the overall topology of the map. Adding the missing connections (eight for each vertex), each decagonal face is seen to be connected to 30 vertices belonging to various other decagonal faces. In this way, the 12 decagonal faces form one single 12-set of interconnected faces, impossible to visualise in 3D space.

For the alternative starting triangle (**1**,**37**,**48**), a similar strategy (calculating images of **1**, **37** and **48** under the twofold operations) leads to the three possible numberings on the right-hand side of figure 7. However, only the solution in the circles survives the test for the images of vertex **1** under the fivefold elements. Addition of the missing edges leads exactly to the structure of figure 6. To see this correspondence, we have added some of the missing edges (dotted edges), which make it possible to see the interior pentagon (**1**,**39**,**20**,**6**,**31**), the quadrangle (**1**,**39**,**18**,**48**) and the triangle (**1**,**37**,**48**).

4.3. The snub dodecahedron

The discussion of the snub dodecahedron can be kept short. As it contains the graph of the small rhombicosidodecahedron as a subgraph and there only existed one such graph, we know that each possible snub dodecahedral subgraph must contain the graph of figure 5 as a subgraph. The only way however to extend this small rhombicosidodecahedral subgraph to a snub dodecahedron is by a triangulation of its 30 quadrangular faces. In principle each quadrangular face can be triangulated in two possible ways, depending on the chosen diagonal, but only one of these triangulations complies with the adjacencies. In fact, the snub dodecahedral structure was implied when we completed the patch of the

small rhombicosidodecahedron (figure 6) and thereby triangulated the squares. The 3D realization based on the unique snub dodecahedral subgraph therefore poses the same problem for visualisation.

4.4. The truncated icosahedron

The last and most interesting subgraph is the truncated icosahedron, corresponding with the framework of Buckminsterfullerene C_{60}. The special relationship of this truncated icosahedral structure to the group PSL(2,11) has already been noted in papers by Kostant. [4, 13, 14] Kostant showed that the graph of C_{60} can be expressed group-theoretically by the structure of a 60-element conjugacy class of PSL(2,11).

In figure 8, we show patches consisting of a pentagon and two hexagons around a common vertex, where by analogy with the small rhombicosidodecahedral case, we can distinguish two starting configurations based on pentagons (**1**, **2**, **3**, **4**, **5**) and (**1**,**31**,**6**,**20**,**39**).

For the case with starting pentagon (**1**, **2**, **3**, **4**, **5**) (figure 8, left), we can use the twofold-axis through the edge separating both hexagons, to find the possible missing neighbour f of vertex **2**. Of the images under the twofold axes (see eq. (9)), only the vertices **24**, **56** and **57** are neighbours of vertex **2**. Owing to the axes through the hexagons, they should however also be images of vertex **1** under some threefold element. By use of eq. (10) we find that this restriction leaves us only with vertex **24** for position f. The truncated icosahedral structure formed by a completion using this trio of generating axes is depicted in figure 9 and can be seen to comply with the adjacency information of table 1. This truncated icosahedral structure will now be used as the backbone for an icosahedral representation of our genus-26 map. It can be completed by adding the eight missing connections for each vertex, following the description of the rotation scheme of table 1. As all 60 vertices are equivalent, we again limit ourselves to the small patch (figure 10) consisting of the pentagon and two hexagons surrounding vertex **2**. From this figure it can be checked that the 11 edges emanating from vertex **2** indeed follow the cyclic rotation described in table 1. Notice,

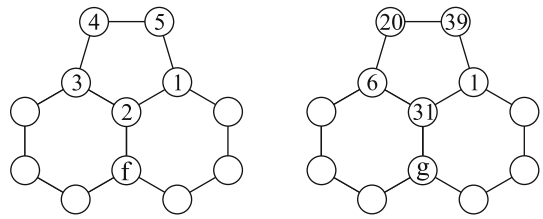

Figure 8. Patches of the truncated icosahedron consisting of all faces surrounding vertex **1** and depicting the cases with starting pentagon (**1**, **2**, **3**, **4**, **5**) (Left) and pentagon (**1**,**31**,**6**,**20**,**39**) (Right).

that different numbers of edges run from vertex **2** to the inside of the two hexagonal cycles, so that addition of the remaining edges has lowered the original I_h symmetry of the truncated icosahedral backbone to the rotational subgroup I. This observation corresponds with the subgroup analysis, which showed only purely rotational icosahedral subgroups. As the genus of our map equals 26, the connections, which run to the insides of the 32 faces of the truncated icosahedron are connected, in such a way as to form 26 handles or tubes. From figure 9, we see that the pentagon (**1**, **2**, **3**, **4**, **5**) and the pentagonal cycle of inscribed vertices (**56**, **57**, **58**, **59**, **60**) correspond to opposite pentagonal faces on the truncated icosahedral backbone. Both pentagonal faces are therefore connected by a single tube or handle formed by the 10 triangles inscribed in the pentagon. The other pairs of opposite pentagons are connected in exactly the same way. The pentagons thus contribute six handles to the total of 26. The remaining 20 handles must originate from the entanglement of the 20 hexagons. To retain icosahedral equivalence of the hexagons, two tubes or handles should leave each hexagon. At first sight, the placement of two tubes per hexagon seems to be incompatible with its local C_3 site-symmetry, but as we shall see this is not necessarily the case. From figure 10, we find that the hexagon (**1–18–17–25–24–2**) is connected to 12 other vertices, which are part of three other hexagons. They are all identified by letters **A** on the Schlegel-diagram of figure 9 and are shown separately in figure 11 together with connections running to their insides. Inspection of these four hexagons shows that they form a closed set in which each hexagon is connected only to the other three. The same holds true for the other 16 hexagons, thereby forming five quartets of hexagons (**A**–**E**), occupying the positions of the five tetrahedra which are hidden in the truncated icosahedron [1]. Each quartet should therefore contribute $20/5 = 4$ to the total genus of the surface. Hence, we obtain 26 as a sum of separate contributions as:

$$26 = 6 + 5 \times 4. \tag{13}$$

To check this, we apply the Euler formula to a spherical truncated icosahedral backbone where only the connections within the **A**-hexagons are completed. All other faces of the backbone are considered closed and without any internal structure, so they will have no influence on the resulting topology. The number of vertices of this structure is 60. For the number of edges and faces we have contributions from the truncated icosahedral backbone and the internal structures of the **A**-hexagons. The number of edges of the backbone is 90 and its contribution to the total number of faces is 28 (32 minus the 4 hexagons). The edges and faces of the internal structure are more difficult to count as some of them show up in two and others in three of the hexagons of figure 11. To simplify the counts, we have shaded the triangular faces which appear three times. They sum up to 24 and therefore correspond to a total of $24/3 = 8$ different triangular faces. All other triangles (48 in total) appear exactly twice and therefore

contribute $48/2 = 24$ to the total number of faces. For the edge-count we find that the edges, which border the shaded faces appear three times; the remaining ones twice. In total this gives us 72/3 + 24/2 = 36 internal edges. Collecting all these results into the Euler equation we get the following result:

$$V - E + F = 60 - (90 + 36) + (28 + 8 + 24) = -6 = 2 - 2g \;\Rightarrow\; g = 4, \quad (14)$$

which proves that a tetrahedral quartet of hexagons indeed contributes 4 to the total genus. In principle it is therefore possible to embed this structure (truncated icosahedral backbone + four interconnecting hexagons) on a surface of genus 4. Giving a satisfying 3D realization of this surface will however be very difficult as there exists no non-self intersecting surface of genus 4 exhibiting at least tetrahedral symmetry. The nearest alternative to realize this symmetry would be to take an icosahedral small stellated dodecahedron,[15] which indeed has the required genus of 4 and icosahedral symmetry but is self-intersecting. Nevertheless, the above analysis has taught us that one can realize the genus-26 map in an icosahedrally symmetrical way. The problem of distribution of 20 handles over the 20 hexagonal faces has been solved by forming five tetrahedral substructures of genus 4. As each face is connected to 4 out of the six vertices of the other three hexagons, each hexagon is connected by $4/6 = 2/3$ of a tube to the other three hexagons of the same set. Although this makes a clear interpretation of the topology more difficult, it gives a solution to the problem of distributing two tubes within the local C_3 symmetry of the hexagon.

Our analysis for the truncated icosahedron is not yet complete, as it remains to investigate the alternative configuration starting with the 5-cycle (**1, 31, 6, 20, 39**). Analysis using eqs. (10) and (11) now results in two solutions (vertex **27** or **37** at position g), which comply with the chosen icosahedral symmetry and can be found in figures 12 and 17. Let us start with the first case and investigate the related patch of figure 13, which shows the complete structure of the map around vertex **31**. A pentagonal cycle no longer combines pairwise with its antipode, but instead connects with two neighbouring vertices of each of its five closest neighbouring pentagons on the truncated icosahedral structure. For instance, vertex **1** is connected to the vertices **18** and **48**, which both belong to the neighbouring pentagon (**18–48–3–51–27**). To visualize these connections, we have thickened the edges between the five vertex-pairs on both figures 12 and 13. As all other pentagons connect in exactly the same way, we end up with one set of 12 mutually connected pentagons. The topology of this set can be again derived by a simple count of vertices, edges and faces. The number of vertices is 60 and the edges and faces arising from the truncated icosahedral backbone are 90 and 20 (32–12), respectively. To count the number of triangular faces, connecting the pentagons, we have once again shaded the faces, which appear three times. All other faces appear twice leading to a total of $120/2 + 60/3 = 80$ triangular faces. In counting the edges resulting from the internal structure one

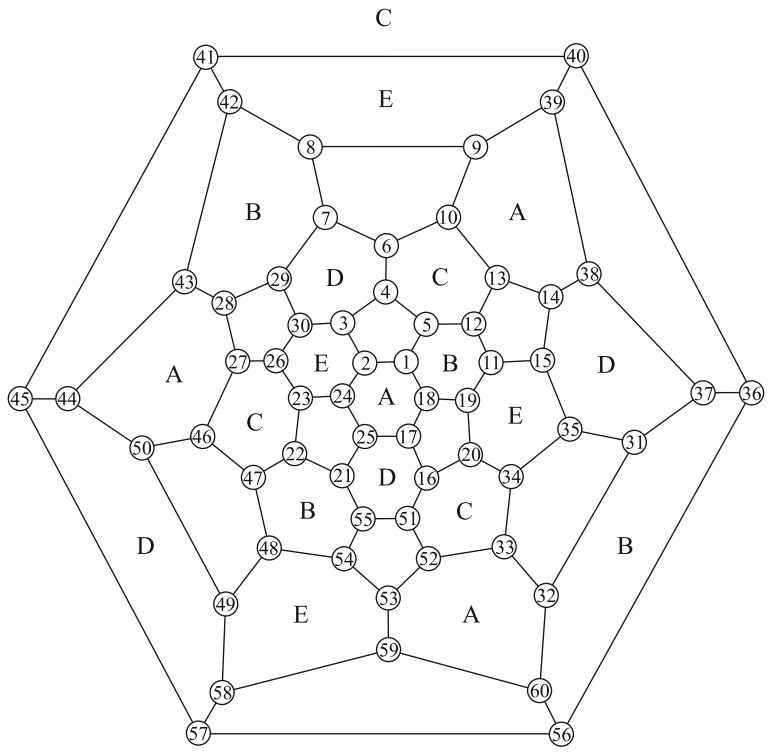

Figure 9. Schlegel diagram of the truncated icosahedral subgraph of the genus-26 dual map found by starting from the pentagonal cycle (**1**, **2**, **3**, **4**, **5**).

must be careful as some edges (indicated in bold in figure 12) have already been counted as edges of the backbone. We thus count $180/3+60/2 = 90$ edges. Using the Euler equation, we have:

$$V - E + F = 60 - (90 + 90) + (20 + 80) = -20 = 2 - 2g \;\Rightarrow\; g = 11. \quad (15)$$

A topology with 11 handles is perfectly justifiable within icosahedral symmetry as it corresponds with that of a "hollow" dodecahedron. It can be seen as a dodecahedral framework where the edges are replaced by tubes, that intersect at the positions of the original vertices. In figure 14 we show this surface by means of a brass artifact dating back to the 2nd century A.D. Several examples have been found all over Europe in archeological sites of the Gallo–Roman period. Their exact use is not known. For our purpose it serves as an icon of a surface of genus 11. Although the structure has 12 holes running through the faces of the dodecahedron, it has genus 11 as the 12th hole is topologically dependent on the others. This can most easily be seen by projecting the surface into a plane, as in figure 15, which indeed shows only 11 holes. To make our analysis concrete, we mapped the 80 interconnecting triangles on this genus-11

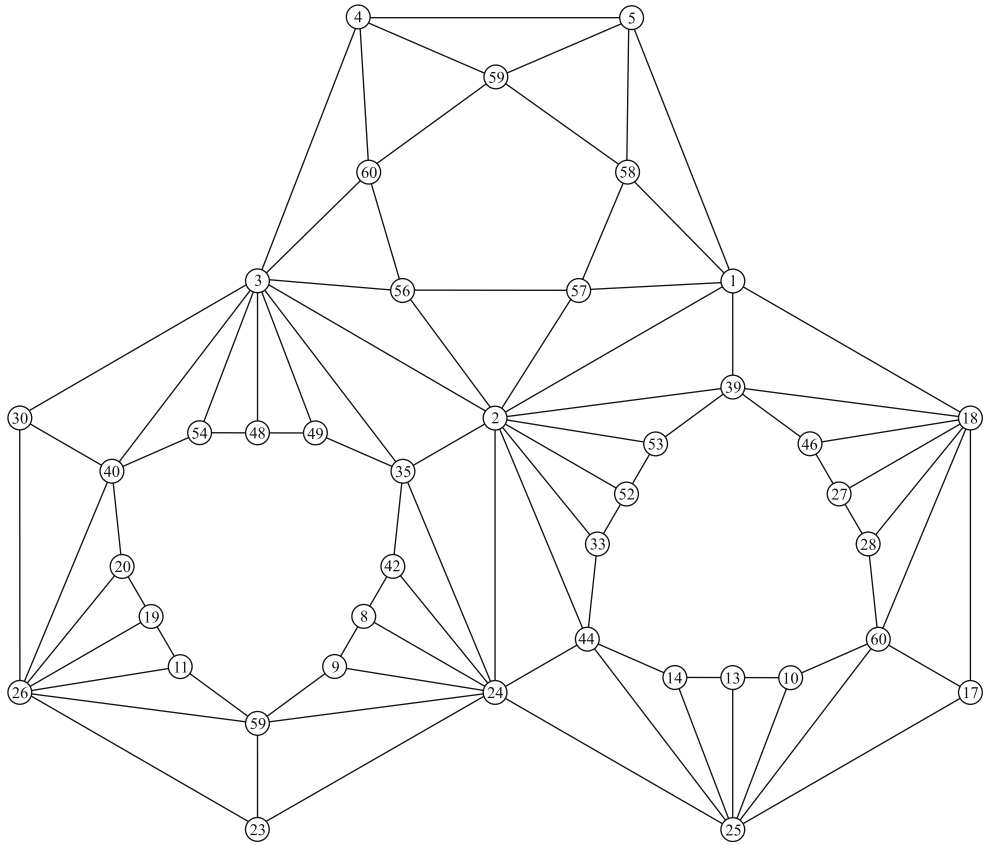

Figure 10. Patch, which visualizes the complete structure of the pentagon and two hexagons surrounding vertex **2**. All other vertices are equivalent and therefore share the same structure.

surface. As the figure shows, each pentagon is surrounded by a ring of 15 triangles. Ten are responsible for the connections between neighbouring pentagons and five, those corresponding to the shaded triangles in figures 12 and 13, form interconnections between 3 mutually neighbouring pentagons, thereby explaining why they appear three times in our previous face-count. As the pentagons of the truncated icosahedral structure consume 11 handles, we are left with 15, which should be evenly distributed among the 20 hexagons. As before, they split into five sets of four interconnecting hexagons, forming five tetrahedral subunits of genus 3 (indicated by letters **A**–**E** in figure 12). The distribution is now:

$$26 = 11 + 5 \times 3. \tag{16}$$

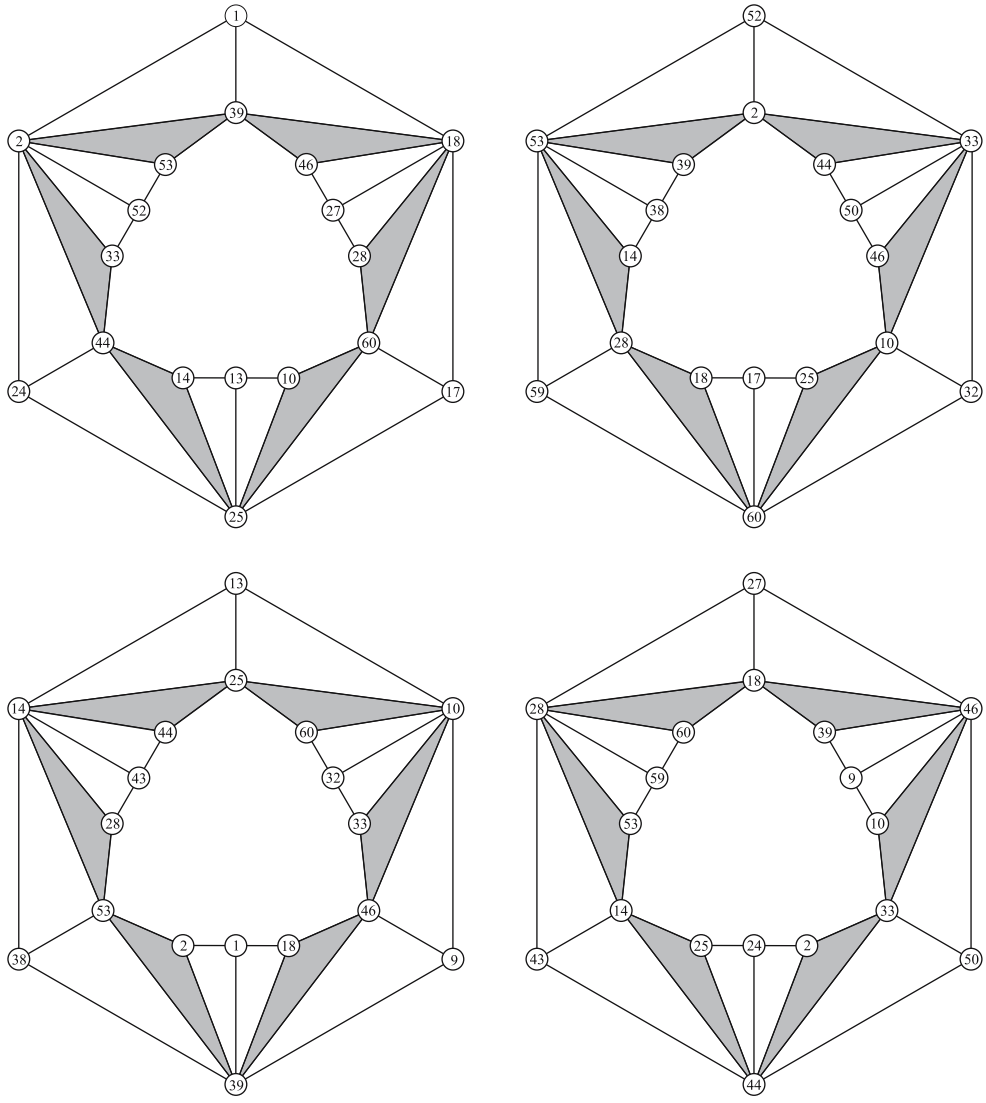

Figure 11. Full visualization of the tetrahedral set of four hexagons, labeled **A**, which connect to each other to form a topology of genus 4. A shading of a triangle indicates that it appears in three out of four hexagons. All other triangles appear twice.

A simple count of the number of vertices, edges and faces gives the following results:

$$\begin{aligned} V &= 60, \\ E &= 90 + 30, \\ F &= 28 + 24 + 4, \end{aligned} \tag{17}$$

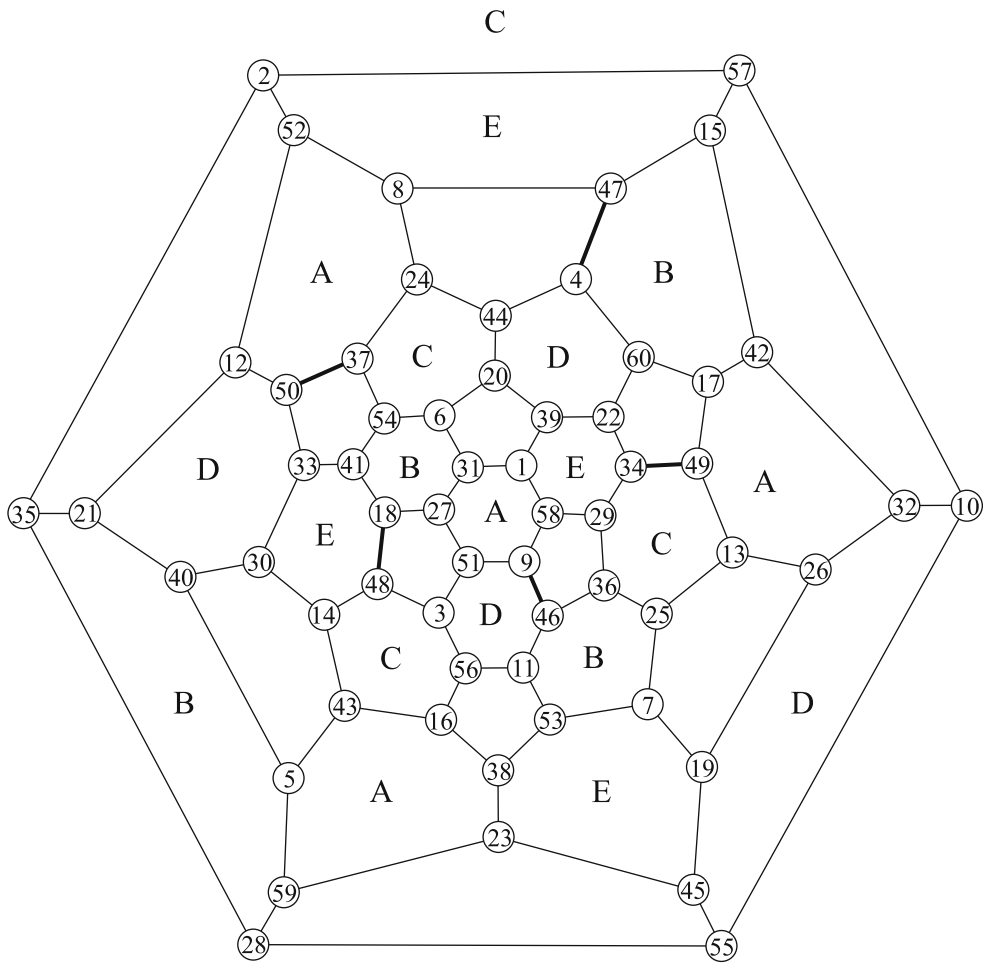

Figure 12. Schlegel diagram of the first truncated icosahedral subgraph of the genus-26 dual map found by starting from the pentagonal cycle (**1**,**31**,**6**,**20**,**39**).

which, by the Euler equation, shows that the four hexagons of a tetrahedral subset do indeed form a topology of genus 3.

$$V - E + F = 60 - 120 + 56 = -4 = 2 - 2g \;\Rightarrow\; g = 3. \tag{18}$$

This genus corresponds with that of a tetrahedral framework of tubes. In figure 16, we give a Schlegel diagram of this surface on which all (220-80)/5=28 triangular faces are embedded. In agreement with figure 13, every hexagon is surrounded by 15 triangles, making the necessary connections to the other three hexagons. The shaded triangles are again located on the meeting points of the tubes and form a bridge between three neighbouring hexagons.

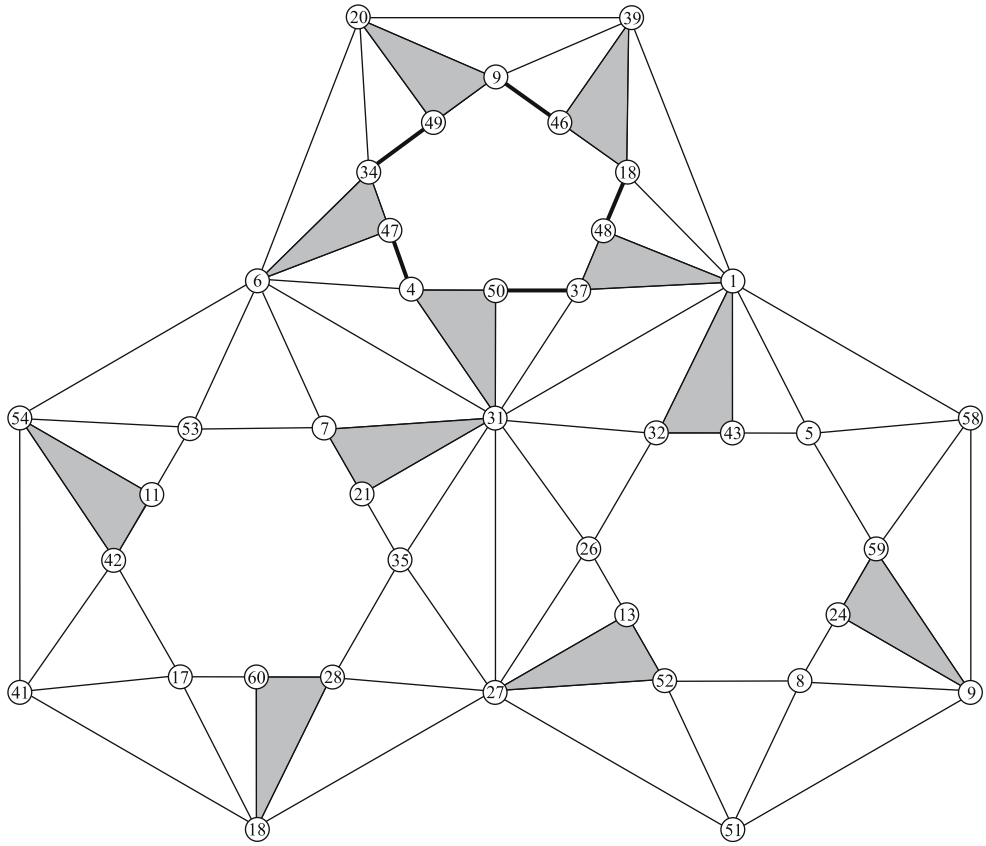

Figure 13. Small patch, taken from the truncated icosahedral subgraph of figure 12 and showing the complete structure of the genus-26 map around vertex **31**.

Figure 14. Brass artifact in the form of a genus-11 hollow dodecahedron dating back to the 2nd century A.D. © Provinciaal Gallo-Romeins Museum, Tongeren, Belgium.

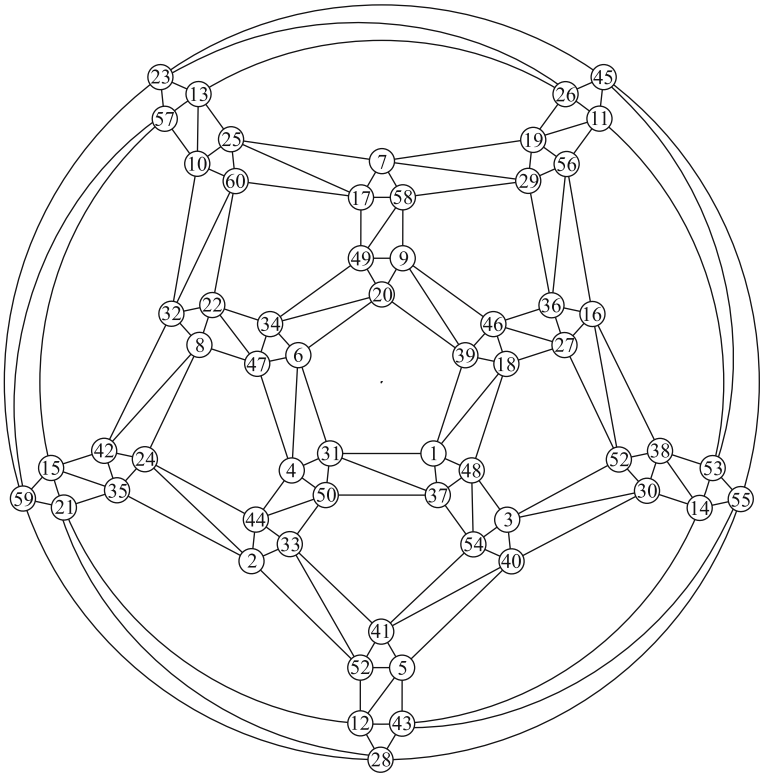

Figure 15. Schlegel diagram of an icosahedral tubular network of genus 11, showing the topology of the set of 12 interconnected pentagons.

Finally, the third and last icosahedral representation of our map (figure 17) leads to no further insight. As we can see from the patch of figure 18, the 20 hexagons are completely tessellated by four triangular faces. As there are no holes running through these hexagons, the 26 handles are completely confined to the set of 12 pentagons and, we have the case:

$$26 = 26 + 0. \tag{19}$$

This corresponds to the realization of figure 6 based on the small rhombicosidodecahedron, and so adds nothing new.

5. A 3-regular carbon network of genus 26

As the 3-regular 220-vertex map and the 11-regular 60-vertex are Poincaré duals to each other, they are topologically equivalent. The topological analysis of the previous section can therefore be used equally well for the 220-vertex map.

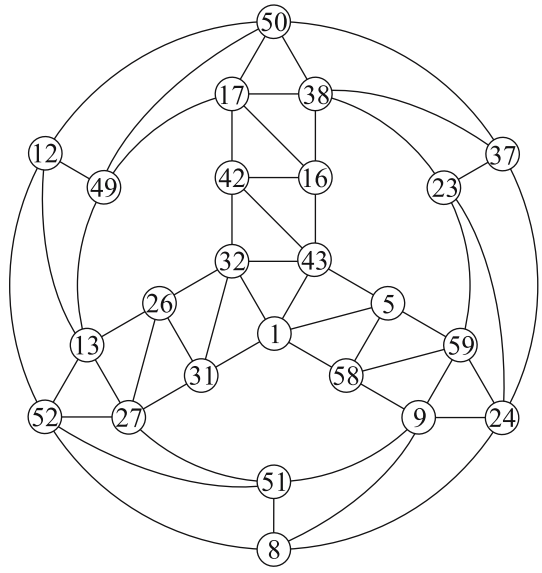

Figure 16. Schlegel diagram of a tetrahedral tubular system of genus 3, showing the topology of the tetrahedral set **A** of four interconnected hexagons.

The most appealing realisation was the case "$26 = 11 + 5 \times 3$" where the handles form a dodecahedral tubular system of genus 11 and five tetrahedral tubular systems of genus 3. As shown in figure 14, the genus-11 tubular system can attain icosahedral symmetry in 3D space in the form of a punctured dodecahedron. The set of five tetrahedral pipeworks can however not comply with icosahedral symmetry: to avoid self-intersection, they have to skirt around each other, thereby inherently lowering the symmetry. A stand-alone icosahedral 3D realisation of the 220-vertex network based on this analysis will therefore be impossible. One plausible way to retain the icosahedral symmetry is to form a hypothetical quasi-crystallographic lattice, leading to a space-filling sp^2 hybridized carbon allotrope consisting of double-shell punctured dodecahedra which are mutually connected by the tubes of the tetrahedral systems of pipes.

6. Independence properties

One mathematical property of relevance to the possible addition chemistry of an sp^2 carbon allotrope is the independence number α of the underlying graph. α is the maximum order of a set of mutually non-adjacent vertices of a graph, and provides a model for the maximum addition of bulky groups to a carbon framework of this topology [16]. A generalisation to d-codes [17] models addends of increasing steric demand: $|C_d|$ is the order of the d-code in the graph, i.e., the maximum order of a set of vertices such that all pairwise dis-

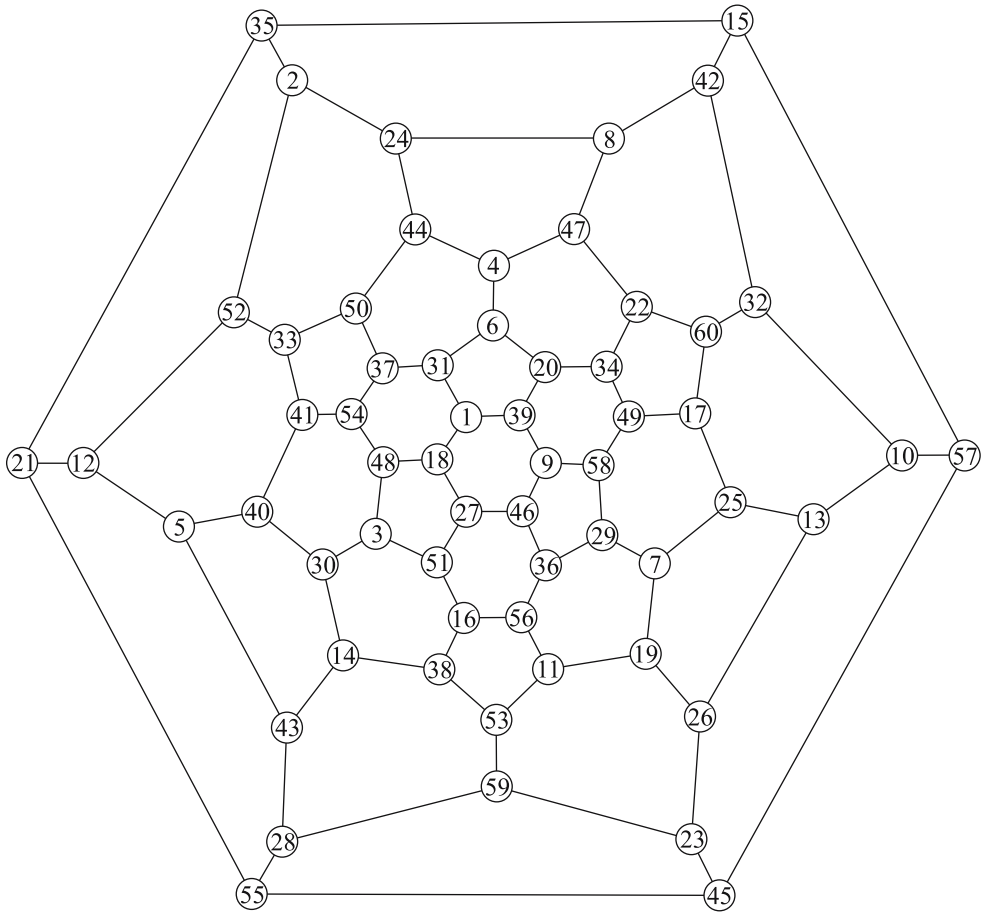

Figure 17. Schlegel diagram of a second truncated icosahedral subgraph of the genus-26 dual map found starting from the pentagonal cycle (**1**,**31**,**6**,**20**,**39**).

tances are at least d. $|C_2|$ is α, representing addends that may not be attached to adjacent sites. If it is required that unfunctionalised vertices support a set of (disconnected) closed-shell π-systems, we have the closed-shell independence number α^-, and generalisations to $d > 2$ [8]. As an 11-gon can support at most five independent vertices our 220-vertex graph has $\alpha \leqslant 5F/3 = 100$ and as the graph is 3-regular, it has $\alpha^- \leqslant 2V/5 = 88$. The graph has diameter (largest pairwise distance) $D = 9$. Direct calculation gives $|C_d|$ for the 220-vertex graph as: 96, 55, 28, 20, 10, 4, 2, 2, 1 for $d = 2, \ldots, 10$, respectively. A carbon allotrope based on the genus-26 map would thus be predicted to support a higher degree of bromination, for example, than C_{60}, for which $\alpha = 24$.

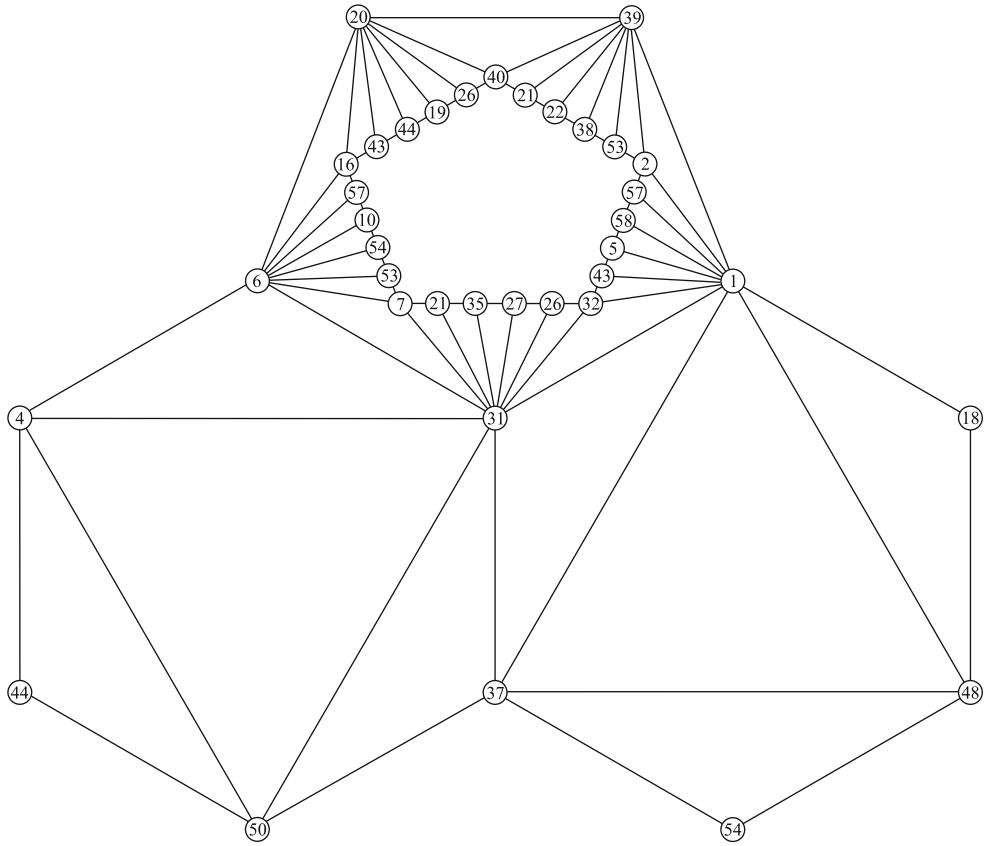

Figure 18. Small patch taken from the truncated icosahedral subgraph of figure 17 and showing the complete structure of the genus-26 map around vertex **31**.

7. Conclusions

The three groups PSL(2,p) with p=5,7 and 11 have special status as permutation groups that act transitively on sets of both orders p and $p+1$. They are also multiples of the rotational symmetry groups of the tetrahedron, octahedron and icosahedron, respectively. Further, they describe the proper symmetries of certain 3-regular maps composed entirely of 5-gons, 7-gons and 11-gons, respectively. The 20-vertex genus-0 map of pentagons is the dodecahedron, the parent of the fullerene family. The 56-vertex genus-3 map of heptagons is the "plumber's nightmare" family of labyrinthine allotropes of carbon. The remaining 220-vertex, genus-26 map of undecagons has been analysed here in terms of the notions of chemical group theory and shown to have a 3D realisation as a punctured truncated icosahedron. The map may serve as a model of an exotic multiply connected sp^2-hybridised carbon network.

Acknowledgments

This work was supported by the Belgian National Science Foundation (FWO-Vlaanderen) and by the Concerted Action Scheme of the Belgian Government. We thank Prof. M. Conder for sending us adjacency details of the 220-vertex map and Prof. W. Myrvold for help with the calculations of the independence numbers. PWF thanks the Royal Society / Wolfson Research Merit Award Scheme for financial support. We thank the Gallo-Roman museum, Tongeren, Belgium for providing the picture of the hollow dodecahedron in figure 14.

References

[1] A. Ceulemans, R.B. King, S.A. Bovin, K.M. Rogers, A. Troisi and P.W. Fowler, J. Math. Chem. 26 (1999) 101–123.
[2] V.S. Kraposhin, private communication, see also V.S. Kraposhin, A.L. Talis and J.M. Dubois, J. Phys: Condens. Matter 14 (2002) 1–10.
[3] R.L. Griess, Jr. and A.J.E. Ryba, Bull. Am. Math. Soc. 36 (1999) 75–93.
[4] B. Kostant, Proc. Natl. Acad. Sci. USA 91 (1994) 11714–11717.
[5] J.H. Conway, R.T Curtis, S.P. Nortin, R.A. Parker and R.A. Wilson, *Atlas of Finite Groups* (Clarendon Press, Oxford, 1985).
[6] F. Klein, Math. Ann. 14 (1879) 428–471.
[7] R.B. King, Discrete Math. 244 (2002) 203–210.
[8] M. Conder and P. Dobcsányi, J. Comb. Math. Comb. Comput. 40 (2002) 41–63.
[9] E. Lijnen and A. Ceulemans, J. Chem. Inf. Comput. Sci. 44 (2004) 1552–1564.
[10] M. Conder and P. Dobcsányi, J. Comb. Theory B 81 (2001) 224–242.
[11] H.S.M. Coxeter and W.O.J. Moser, *Generators and Relations for Discrete Groups*, 3rd edn (Springer-Verlag, Berlin, 1972).
[12] M.R. Garey and D.S. Johnson, *Computers and Intractibility: A Guide to the Theory of NP-Completeness* (W.H. Freeman and Co., San Francisco, CA, 1979).
[13] B. Kostant, Not. Am. Math. Soc. 42 (1995) 959–968.
[14] B. Kostant, Sel. Math. New. Ser. 1 (1995) 165–195.
[15] H.S.M. Coxeter, *Regular Polytopes*, 3rd edn (Dover Publications, New York, 1973).
[16] P.W. Fowler, P. Hansen, K.M. Rogers and S. Fajtlowicz, J. Chem. Soc. Perkin Trans. 2, (7) (1998) 1531-1533.
[17] P.W. Fowler, B. de La Vaissière and M. Deza, J. Mol. Graph. Model 19 (2001) 199–204.
[18] P.W. Fowler, K.M. Rogers, K.R. Somers and A. Troisi, J. Chem. Soc. Perkin Trans. 2, (10) (1999) 2023–2027.